Artificial
Organs

Copyright © 2014 International Center for Artificial Organs and Transplantation and Wiley Periodicals, Inc.

# Thoughts and Progress

## Multilaboratory Study of Flow-Induced Hemolysis Using the FDA Benchmark Nozzle Model

*Luke H. Herbertson, †Salim E. Olia, †Amanda Daly, ‡Christopher P. Noatch, ‡§William A. Smith, †¶Marina V. Kameneva, and *Richard A. Malinauskas
*Center for Devices and Radiological Health, US Food and Drug Administration, Silver Spring, MD; Departments of †Bioengineering and ¶Surgery, University of Pittsburgh, Pittsburgh, PA; ‡Lerner Research Institute, Cleveland Clinic; and §Engineering Department, Perfusion Solutions, Inc., Cleveland, OH, USA

**Abstract:** Multilaboratory in vitro blood damage testing was performed on a simple nozzle model to determine how different flow parameters and blood properties affect device-induced hemolysis and to generate data for comparison with computational fluid dynamics-based predictions of blood damage as part of an FDA initiative for assessing medical device safety. Three independent laboratories evaluated hemolysis as a function of nozzle entrance geometry, flow rate, and blood properties. Bovine blood anticoagulated with acid citrate dextrose solution (2–80 h post-draw) was recirculated through nozzle-containing and paired nozzle-free control loops for 2 h. Controlled parameters included hematocrit (36 ± 1.5%), temperature (25°C), blood volume, flow rate, and pressure. Three nozzle test conditions were evaluated ($n$ = 26–36 trials each): (i) sudden contraction at the entrance with a blood flow rate of 5 L/min, (ii) gradual cone at the entrance with a 6-L/min blood flow rate, and (iii) sudden-contraction inlet at 6 L/min. The blood damage caused only by the nozzle model was calculated by subtracting the hemolysis generated by the paired control loop test. Despite high intralaboratory variability, significant differences among the three test conditions were observed, with the sharp nozzle entrance causing the most hemolysis. Modified index of hemolysis ($MIH_{nozzle}$) values were 0.292 ± 0.249, 0.021 ± 0.128, and 1.239 ± 0.667 for conditions i–iii, respectively. Porcine blood generated hemolysis results similar to those obtained with bovine blood. Although the interlaboratory hemolysis results are only applicable for the specific blood parameters and nozzle model used here, these empirical data may help to advance computational fluid dynamics models for predicting blood damage. **Key Words:** Hemolysis—Red blood cell damage—Nozzle model—Fluid dynamics—In vitro hemolysis testing—Computational fluid dynamics.

Many blood-contacting medical devices, including prosthetic heart valves, catheters, blood pumps, and cardiopulmonary bypass oxygenators, can cause blood cell damage (1–4). Hemolysis, which is characterized by the release of intracellular hemoglobin from damaged red blood cells (RBCs) into the surrounding plasma, can lead to serious clinical sequelae such as anemia, hypertension, smooth muscle dystonia, arrhythmias, thrombosis, and renal failure (5). To address these potential adverse effects, manufacturers must demonstrate that their cardiovascular devices do not cause excessive blood damage before they can be marketed. Typically, device safety in terms of blood damage potential is demonstrated through dynamic in vitro hemolysis testing. This usually involves recirculating animal blood through a subject device for a defined duration under clinically relevant flow and pressure conditions and measuring the amount of resulting hemolysis in relation to that caused by a similarly tested, already marketed device (6,7). As many factors, including blood species, temperature, and preparation (e.g., anticoagulation, storage, and blood age), can affect generated hemolysis (8), it is difficult to compare in vitro test results from different laboratories and extrapolate them to clinical outcomes.

While the use of computational fluid dynamics (CFD) modeling is now commonplace for device design, adoption of predictive flow-related blood damage models requires extensive experimental validation. Empirical studies using various flow models (e.g., orifice plate creating a submerged jet, cone-and-plate viscometer, Couette rheometer, capillary tube) have shown that flow-related blood damage is a function of both shear stress and time of exposure to fluid forces (9–13). Constitutive equations generated by these studies have been incorporated into computational models to predict hemolysis (14) and platelet damage (15) and have been utilized

doi:10.1111/aor.12368

Received January 2014; revised May 2014.

Address correspondence and reprint requests to Dr. Luke Herbertson, US Food and Drug Administration—Center for Devices and Radiological Health, 10903 New Hampshire Ave., Office of Science and Engineering Laboratories, WO 62, Room 2120 Silver Spring, MD 20993, USA. E-mail: luke.herbertson@fda.hhs.gov

in the development of a variety of medical devices (16,17). However, CFD predictions of blood damage are heavily dependent on which empirical shear-stress exposure time model is used and how it is implemented (17,18).

CFD analyses are not required in device premarketing applications to the US Food and Drug Administration (FDA), but they are increasingly being used as a complementary tool in premarket device evaluation and postmarket forensic investigations. As part of an FDA initiative to evaluate the utility of CFD for assessing medical device safety and to understand the limitations of CFD in this field, in vitro blood damage testing was performed on a simple nozzle model to generate interlaboratory data for comparison with computational predictions. The focus of this particular study is not on CFD analytical techniques, but rather on the importance of the experimental data needed to validate computational models. Current limitations in experimental hemolysis studies have included the following: (i) not accounting for important differences in RBC fragility between species in various flow regimes (19,20); (ii) not implementing realistic times of RBC exposure to high stresses (usually less than 1 s) during the in vitro testing; (iii) not addressing how blood collection and test conditions such as the source of animal blood, drawing technique, anticoagulation, time after withdrawal, temperature, and pH may affect flow-induced hemolysis (8); (iv) not disclosing important details about the models (e.g., surface roughness and corner contours) (21); and (v), failing to adequately verify experimental hemolysis results among multiple laboratories (22).

In this study, three independent laboratories conducted in vitro hemolysis experiments on a reversible nozzle model to relate physical parameters (e.g., flow rate, device geometry, and animal blood properties) to RBC trauma. To our knowledge, this is the first multilaboratory study to comparatively evaluate in vitro hemolysis in the same specific test model. A multilaboratory assessment is beneficial in that it draws on expertise from multiple sources, incorporates real world testing biases, and can provide large sample sizes that may be impractical to obtain from a single center. Complementary interlaboratory studies that describe the flow field characteristics in this nozzle model using particle image velocimetry measurements (23) and computational simulations (24,25) under slightly different flow conditions are publicly available at https://fdacfd.nci.nih.gov to encourage further improvements in the development and evaluation of medical device blood damage models using computational simulation tools.

## MATERIALS AND METHODS

### Nozzle model

The FDA benchmark nozzle model, which forces blood from a tube with a 12-mm inner diameter into a throat region with a 4-mm inner diameter (40 mm long), was based on earlier nozzle model designs that were shown to induce measurable hemolysis (26,27). The nozzle model contains regions of sudden and gradual changes in cross-sectional area, similar to many actual blood-contacting medical devices (e.g., catheters, syringes, hemodialysis tubing, oxygenators, and hypodermic needles). Figure 1 displays the

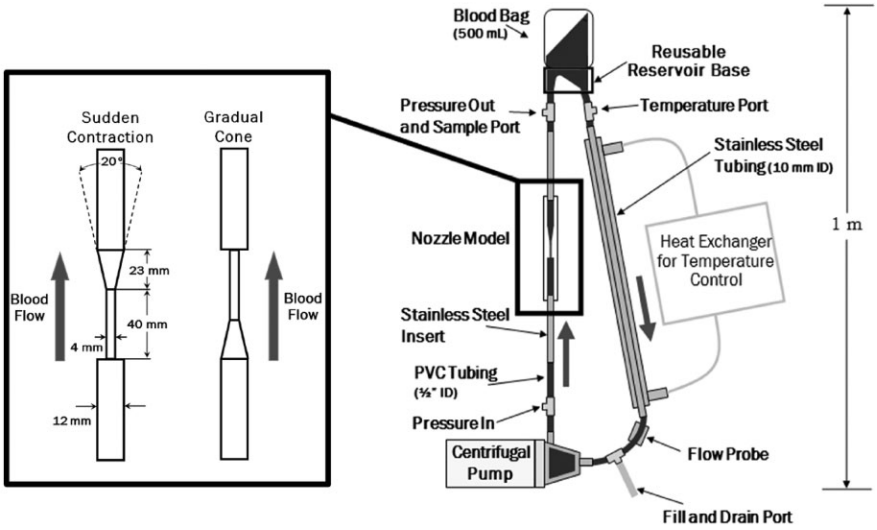


**FIG. 1.** Nozzle model design (left) and schematic of the recirculating blood damage test loop (right). The model was evaluated with a sudden contraction at the entrance to the throat at flow rates of 5 and 6 L/min and with a gradual cone inlet configuration at 6 L/min.

critical dimensions, along with the two flow orientations of the test model (on the left): (i) with a sharp-cornered sudden contraction at the inlet to the nozzle throat at blood flow rates of 5 and 6 L/min, and (ii) with the model reversed such that the gradual conical section was at the inlet to funnel blood into the stenotic throat at 6 L/min. Three identical nozzle models were fabricated in blocks of acrylic ($2.5 \times 2.5 \times 16.5$ cm) through a process of milling, hand-polishing, vapor-polishing, and temperature annealing. Since rough surfaces ($R_a > 0.6$ μm) are more likely to contribute to hemolysis (13,21,28), smooth blood-contacting surfaces were maintained throughout the nozzle model and flow loop. These surfaces were assessed using a stereomicroscope and metrology rubber (Reprorubber, Flexbar Machine Corp., Islandia, NY, USA), a profile optical comparator (PH-350, Mitutoyo, Aurora, IL, USA), and an optical surface profilometer (ContourGT-K1, Bruker AXS, Madison, WI, USA). The models conformed to the following geometrical parameters: (i) an inlet diameter of $12.00 \pm 0.13$ mm with a throat diameter of $4.00 \pm 0.08$ mm; (ii) an angle of sudden contraction of $90.0 \pm 0.1°$; (iii) a radius of curvature at sudden contraction corner <25 μm; (iv) angle of gradual cone of $20 \pm 1°$; (v) misalignment of the cone geometry from the center of the tube <0.03 mm; and (vi) surface roughness $R_a < 0.3$ μm with no visible tool marks on the blood-contacting surfaces. Polished stainless steel tubes (12-mm inner diameter, 15-cm length, $R_a < 0.3$ μm) were sealed using polytetrafluoroethylene thread tape into countersinks on both sides of the acrylic model to maintain undisturbed entry and exit flow (~19 cm long) to and from the nozzle throat section. To account for any possible geometric or surface discrepancies among the three nozzle models, each model was tested by each laboratory.

**Test circuit**

The flow loop shown in Fig. 1 was standardized to conduct sensitive and reproducible in vitro hemolysis testing using a magnetically levitated centrifugal blood pump (Levitronix, Waltham, MA, USA) to recirculate the blood. Blood from the pump outlet entered a straight section of half-inch-inner-diameter Tygon S-50-HL medical grade tubing (St. Gobain, Akron, OH, USA), which connected to the vertically mounted nozzle model. A vertical configuration was used to assist in circuit priming and to match the previous velocity characterization experiments (23). Pressure drop was measured across the model with digital pressure transducers (Digimano 1000, Netech, Farmingdale, NY, USA, or Model 1502B01EZ5V20GPSI, PCB Piezotronics, Depew, NY, USA). Blood samples were acquired from a low-pressure stopcock port distal to the nozzle outlet. The reservoir was designed to increase test sensitivity by minimizing blood volume, to promote blood mixing and minimize stagnation zones, and to withstand collapse from low pump inlet pressures while maintaining a closed system. The reservoir was composed of a 500-mL medical-grade PVC bag (Qosina, Edgewood, NY, USA) with a sealable air vent. The bag was cut and clamped over an acrylic reservoir base with blood inlet and exit ports with half-inch outer diameters, and it was heat-sealed diagonally to reduce the loop volume and facilitate blood mixing. Each experiment used an average blood volume of 275 or 295 mL, depending on the test site.

A thin-walled stainless steel tube (10-mm inner diameter, 50 cm long) enclosed within a water jacket was used as an intraluminal heat exchanger to maintain a blood temperature of $25.0 \pm 1.5°C$. A clamp-on 9XL ultrasonic flow probe and meter (T110R, Transonic Systems, Inc., Ithaca, NY, USA), factory-calibrated with blood and regularly calibrated on site with phosphate-buffered saline (PBS) or blood, were used to monitor blood flow rate. Lastly, an access port was located at the bottom of the loop to allow draining and refilling of the system between tests.

**Blood preparation and quality assessment**

For hemolysis testing, the three laboratories used bovine blood obtained from commercial donor animals or from an abattoir. To determine whether blood species could affect the results, two of the groups later repeated a subset of the test conditions using porcine blood. Donor blood was drawn from live animals via venipuncture using a 12-G lancet and arrived at the testing facility within 24 h of being drawn. Abattoir blood was obtained immediately after death using venipuncture as described above or gravity-collected into a bucket after vascular incision and arrived at the test site within 1.5 h of the draw. Each blood pool was used for two consecutive days of testing, and all testing was completed within 80 h of the blood being drawn. The blood was stored at 4°C when not in use. Each laboratory used a total of six distinct blood pools to complete the testing with bovine blood.

Anticoagulation was achieved using a 1:8 ratio of acid citrate dextrose solution A (ACDA) to blood. ACDA was used in this study due to its ability to effectively preserve blood cells over multiple days of storage (29). For each multiple-day test, 4 L of blood was filtered through a latex-free mesh (40–75 μm pore

size) and pooled together at the test facility. Hematocrit was determined by centrifugation of standard capillary tubes and adjusted to 36.0 ± 1.5% by either hemodilution with PBS or hemoconcentration through plasma removal. The blood was gently mixed prior to loading into the test loop.

Blood quality was assessed by monitoring the baseline hemolysis level of the normalized blood pool and by a rocker bead test, which was used to characterize RBC mechanical fragility for each separate blood pool on each day of testing (30,31). For the RBC mechanical fragility test, five 7-mL test tubes (silicone-coated glass; Becton Dickinson Vacutainer, Fisher Scientific, Franklin Lakes, NJ, USA) were utilized such that three test tubes contained five stainless steel ball bearings each (1/8″ diameter, BNMX-2 Type 316 SS balls, Small Parts, Miami Lakes, FL, USA), while the remaining two test tubes contained no ball bearings and served as controls. Each tube was filled with 3 mL of blood, placed on a platform rocker (M79700 Platform Vari-Mix Rocker, Barnstead Thermolyne Corp., Dubuque, IA, USA), and rocked for 1 h at 18 cycles per minute with a 17° oscillatory amplitude. After 1 h, plasma free hemoglobin concentration (fHb) was measured in each sample. The RBC mechanical fragility index (MFI), shown in Eq. 1, was used as a measure of RBC mechanical fragility (30):

$$\mathrm{MFI} = \frac{\mathrm{fHb_{final}} - \mathrm{fHb_{control}}}{\mathrm{tHb_{pool}} - \mathrm{fHb_{control}}} * 100 \qquad (1)$$

where $\mathrm{fHb_{final}}$ is the plasma free hemoglobin concentration (mg/dL) in the samples with beads, $\mathrm{fHb_{control}}$ is the hemolysis level (mg/dL) in the rocked control samples without beads, and $\mathrm{tHb_{pool}}$ is the total hemoglobin concentration (mg/dL) of the pooled blood.

Blood viscosity was measured each test day at a shear rate of 200 $s^{-1}$ using a cone-and-plate rheometer (Brookfield, Middleboro, MA, USA) or an oscillatory viscometer (Vilastic-3, Vilastic Scientific, Austin, TX, USA). Density was calculated by weighing 100 mL of blood, and plasma protein concentration was measured with a refractometer (TS 400, Reichert, Depew, NY, USA). All three laboratories measured the pH levels of the blood. Additionally, two laboratories measured carbon dioxide and oxygen levels with a blood gas analyzer and blood glucose concentrations using a glucometer (Hemocue, Glucose 201 Analyzer, Cypress, CA, USA).

**Flow conditions**

The Reynolds number (Re) in the throat of the model was calculated as

$$\mathrm{Re} = \frac{4\rho Q}{\pi \mu D} \qquad (2)$$

where ρ is the density of blood, $Q$ is the measured blood flow rate, μ is the dynamic viscosity of blood, and $D$ is the 4-mm throat diameter of the model. Initially, our intent was to study blood flow at Reynolds numbers ranging from 500 to 6500 to correlate hemolysis levels with (i) the shear stresses estimated using particle image velocimetry in similarly prepared acrylic nozzle models (23) and (ii) the hemolysis predictions obtained through computational simulations (24). In the companion particle velocimetry study (23), the authors evaluated flow through the FDA nozzle model for throat Reynolds numbers that corresponded to a blood flow rate range of 0.4–5.0 L/min. This flow range encompassed both laminar and turbulent flow regimes. However, preliminary hemolysis testing with the nozzle model revealed that blood cell damage was minimal when the flow rate was below 5 L/min, so low flow rates were excluded from hemolysis testing. When the flow rate exceeded 6.5 L/min, flow-induced cavitation could be acoustically detected at the sudden-contraction entrance to the throat region using a hydrophone (Model 132A32, PCB Piezotronics) with a signal conditioner (Model 480C02, PCB Piezotronics). Since differentiation between shear-induced blood damage and cavitation-related hemolysis would not be possible, the nozzle model was operated below the cavitation threshold with testing only performed at 5 and 6 L/min.

**Experimental procedure**

Hemolysis testing involved the alternation of the nozzle model between two identical flow loops that were operated simultaneously. For each nozzle model experiment, a corresponding control test preceded or followed that matched pressure and flow conditions using the same blood pool, test loop, and blood pump. In a few cases, a single control loop corresponded to two distinct nozzle-containing test loops. For the control experiments, the acrylic model and stainless steel extensions were removed and replaced with two polycarbonate reducers (1/2″ to 1/4″), a 30″ looped segment of Tygon S-50-HL medical grade tubing 1/4″ in inner diameter, and an adjustable hosecock clamp. The baseline control tests were used to compensate for the blood damage caused by the flow loop components (e.g., the pump, connectors, reservoir, and tubing) other than the nozzle. To isolate the blood damage caused by the nozzle model itself at a specific flow condition, the free hemoglobin values generated by the baseline

control loop were subtracted from the results of the corresponding nozzle test loop. To differentiate between the 6-L/min control loops, the baseline control corresponding to the nozzle conical inlet direction is referred to as "Control A," and that for the sudden-contraction entrance is "Control B."

PBS was recirculated through each of the flow loops for 15 min prior to the beginning of the blood tests to wet the blood-contacting surfaces. The PBS was then drained, and blood was gravity-filled from the lowest point in the loop to minimize mixing with air. The blood was allowed to circulate for 5 min at a flow rate <2 L/min to de-air the system before the start of each test. Each experiment lasted 2 h with blood samples drawn every 40 min. One milliliter of blood was withdrawn from the sampling port and discarded before two 2-mL blood samples were drawn for analysis.

A standardized cleaning protocol was established to reduce procedural discrepancies among the laboratories. At the start of each test day, new reservoir bags and tubing sets were used. In between same-day experiments, the loop was washed twice with fresh PBS to remove any visible trace of blood. At the end of each test day, the acrylic nozzle model, stainless steel extensions, heat exchanger, pump head, and acrylic reservoir base were rinsed with PBS, washed with soap/degreaser (Versa-Clean, 10× dilution, Fisherbrand, Pittsburgh, PA, USA; or 1% Simple Green, Sunshine Makers, Inc., Huntington Beach, CA, USA) and water, then washed with 70% isopropanol or ethanol, rinsed with deionized water, and allowed to completely dry before reassembly with new tubing. No metal brushes were used during the cleaning process to avoid scratching the blood-contacting surfaces. Pump heads were replaced after 2 consecutive days of testing.

**Hemolysis assays and analysis**

To prepare plasma for analysis, blood samples were first centrifuged at no more than $2000 \times g$ for 15 min, followed by plasma isolation and recentrifugation at $13\,000 \times g$ for 15 min. Using the resulting supernatant plasma, hemolysis was determined spectrophotometrically by measuring the change in fHb. The Cripps method (32), used by all three laboratories to quantify hemolysis, is based on the oxyhemoglobin levels at three wavelengths (560, 576.5, and 593 nm) as shown below (33):

$$\mathrm{fHb}\{\mathrm{mg/dL}\} = (\mathrm{conv}) * \left[ A_{576.5\,\mathrm{nm}} - \frac{A_{560\,\mathrm{nm}} + A_{593\,\mathrm{nm}}}{2} \right] * (\mathrm{dil}) \quad (3)$$

where 'conv' refers to the spectrophotometer conversion factor and 'dil' is the dilution factor of the sample. The conversion factor, determined by calibration of the spectrophotometer with serial dilutions of hemoglobin standards, was approximately 177.6 for all of the spectrophotometers used in this study (33). To ensure that measurements were made within the linear range of the spectrophotometer, fHb values above 150 mg/dL were diluted with PBS and re-measured. Prior to conducting the nozzle hemolysis study, stock fHb solutions were distributed, and all laboratories measured within ±3.5 mg/dL of target values ranging from 0–100 mg/dL (i.e., <3.6% coefficient of variation). As multiple blood samples were assayed over the 2-h loop tests, all ΔfHb values were based on a linear regression analysis of the slope of the fHb versus time plots using eight measurements taken over four sampling times.

To account for variations in the test parameters (e.g., flow rate, blood volume, hematocrit, and total blood hemoglobin concentration) between experiments, the measured fHb was normalized by calculating the normalized index of hemolysis (NIH) (22).

$$\mathrm{NIH}\{\mathrm{g/100L}\} = \Delta\mathrm{fHb} * V * \frac{100 - \mathrm{Hct}}{100} * \frac{1}{Q * t} \quad (4)$$

where $V$ is the volume of blood in the flow system (L), $Q$ is the blood flow rate (L/min), Hct is the hematocrit of the blood (%), and $t$ is the duration of the test (min). The modified index of hemolysis (MIH) can be derived from the NIH and accounts for the total hemoglobin concentration in the blood (tHb, mg/dL) (8).

$$\mathrm{MIH}\{\mathrm{mg/mg}\} = \mathrm{NIH} \times \frac{10^6}{\mathrm{tHb}} \quad (5)$$

MIH is reported in dimensional units of milligrams of hemoglobin released into plasma divided by the milligrams of total hemoglobin pumped through the loop (6). To minimize decimal places, a constant factor of $10^6$ is used (8). To account for the hemolysis caused solely by the nozzle model ($\mathrm{MIH_{nozzle}}$), the MIH value measured in the matched control loop ($\mathrm{MIH_{control}}$) was subtracted from the blood damage caused by the nozzle test loop ($\mathrm{MIH_{test}}$) according to Eq. 6.

$$\mathrm{MIH_{nozzle}} = \mathrm{MIH_{test}} - \mathrm{MIH_{control}} \quad (6)$$

**Sample size and statistical analysis**

Hemolysis data were collected on two adjacent days for each blood pool, resulting in an uneven

number of repeats for the three test conditions. Specifically, the sudden-contraction nozzle inlet condition at 6 L/min had 36 total repeats, whereas only 27 repeats were collected for each of the other two nozzle test conditions. The number of repeats was sufficient to assess experimental reproducibility (including intraday repeatability) and the effect of blood aging between test days.

Statistical analyses were performed using unpaired *t*-tests, and a *P* value of less than 0.05 was considered statistically significant. When multiple conditions were compared, an *F*-test was first performed to detect differences between groups. Linear regression coefficients were used to quantify the variability of the results and the linear association of the hemolysis data with the test duration and other test parameters. The standard deviation (SD) and percentage coefficient of variation (% CV = SD/mean times 100%) were reported to indicate the variability of the results at a given condition. Grubbs' extreme studentized deviate test was used to detect outliers in the data set. Additionally, to estimate the contribution of viscosity, flow rate, and density measurement uncertainties towards the overall variability in the hemolysis data, an error propagation analysis was performed using commercial CFX software (ANSYS, Inc., Canonsburg, PA, USA) and a modified Grigioni (Lagrangian) blood damage model (34) with Giersiepen–Wurzinger constants (35) in MATLAB (MathWorks, Natick, MA, USA).

## RESULTS

The chemical and physical properties of bovine and porcine blood after hematocrit adjustment to 36% are shown in Table 1. In general, the measured blood properties were similar for each laboratory and independent of the blood source (i.e., live donor or abattoir), method of blood collection (i.e., venipuncture vs. bucket), and storage age of the blood at the start of each experiment (i.e., 3–80 h old). While the daily order in which the experiments were performed was inconsequential, the blood storage time (e.g., first day of testing vs. second day) did have a significant effect on the dynamic hemolysis test results. When the same test condition was run on consecutive days, hemolysis levels were higher on the second test day compared with the first by about 20% ($n = 18$, $P < 0.03$). In spite of this difference, the hemolysis results for the three laboratories have been collated based on test condition irrespective of test day, as each test condition was evaluated an equal number of times on both days.

The effects of device geometry and flow rate on hemolysis were studied under three test conditions: (i) sudden-contraction nozzle inlet at 5 L/min, (ii) gradual cone inlet at 6 L/min, and (iii) sudden-contraction inlet at 6 L/min. The hemodynamic operating conditions for each lab were comparable with mean blood flow rates, all being within 0.2 L/min, or ~4%, of the target values of 5 and 6 L/min. The measured pressure drops across the nozzle models were also similar among the laboratories (5–7% CV). Pressure drop variations among the laboratories were attributed to pump speed discretization (±100 rpm) and to calibration differences in the flow and pressure probes. Table 2 shows that the target flow rates of 5 and 6 L/min equated to turbulent nozzle throat Reynolds numbers of $6650 \pm 570$ and $7950 \pm 660$, respectively. At both flow rates, the flow in the half-inch-inner-diameter tubing of the loop was transitional in nature ($R_e = 2220 \pm 190$ and $2670 \pm 220$ for 5 and 6 L/min, respectively). Based on mean velocities, the average exposure time of an RBC to the throat region was 5 to 6 ms for the 6- and 5-L/min flow rates, respectively.

The average initial fHb value at the start of all dynamic hemolysis tests with bovine blood was $15.5 \pm 7.3$ mg/dL. During hemolysis testing, the fHb increased linearly over the duration of the experiment as shown in Fig. 2 (e.g., $r^2 > 0.94$ for sudden-contraction nozzle inlet at 6 L/min for the 12 repeats from one laboratory). The fHb magnitude and linearity indicate that a 2-h experimental run

**TABLE 1.** *Physical and chemical properties of the bovine and porcine blood adjusted to 36% hematocrit*

| Blood species | Original hematocrit (%) | Adjusted hematocrit (%) | Density (g/mL) | Viscosity at 25°C (cP)‡ | Plasma protein (g/dL) | Total hemoglobin (g/dL) | Glucose (mg/dL) | pH at 37°C | $pO_2$ (mm Hg) | $pCO_2$ (mm Hg) | Blood fragility |
|---|---|---|---|---|---|---|---|---|---|---|---|
| Bovine* | 38.0 ± 2.2 | 36.2 ± 1.1 | 1.04 ± 0.01 | 4.21 ± 0.32 | 6.5 ± 0.6 | 11.9 ± 0.8 | 365 ± 59 | 6.82 ± 0.10 | 71 ± 23 | 87 ± 21 | 0.54 ± 0.15 |
| Porcine† | 44.4 ± 2.9 | 36.4 ± 0.8 | 1.04 ± 0.01 | 4.06 ± 0.58 | 6.8 ± 0.6 | 11.6 ± 0.9 | — | 6.81 ± 0.10 | 56 ± 32 | 86 ± 10 | 0.42 ± 0.06 |

Values are shown as mean ± SD. * Values for bovine blood were based on data taken from three laboratories ($n = 36$ for all parameters except plasma protein, glucose, and blood gases, for which $n = 18$ to 28). † Porcine blood properties were measured in two laboratories ($n = 16$ for all parameters except glucose and blood gases, for which $n = 4$ to 12). The glucose concentration in porcine blood anticoagulated with acid citrate dextrose solution A was not reported, as it often exceeded the measurable range of the glucose analyzer. ‡ Viscosity of bovine and porcine blood was measured at a shear rate of 200 $s^{-1}$.

**TABLE 2.** *Flow parameters in the nozzle model for the three test conditions*

| | Sudden-contraction inlet, 5 L/min ($n$ = 26) | Gradual cone inlet, 6 L/min ($n$ = 26) | Sudden-contraction inlet, 6 L/min ($n$ = 36) |
|---|---|---|---|
| Measured flow rate (L/min) | 5.05 ± 0.12 | 5.94 ± 0.14 | 6.07 ± 0.08 |
| Pressure drop across nozzle model (mm Hg) | 217 ± 15 | 309 ± 22 | 297 ± 15 |
| Pump speed (rpm) | 3420 ± 70 | 4020 ± 110 | 3970 ± 60 |
| Reynolds number in nozzle throat | 6650 ± 570 | 7860 ± 640 | 8020 ± 670 |
| Reynolds number in half-inch-inner-diameter tubing | 2220 ± 190 | 2630 ± 210 | 2670 ± 220 |

Values are shown as mean ± SD for three laboratories combined.

time was sufficient to generate blood damage with the nozzle model and that autohemolysis was not a likely factor during the tests. However, Fig. 2 also illustrates the variability in hemolysis test results when 12 experiments were performed on different days with different pools of blood; the variability in slope of the hemolysis versus time plots was 47% CV.

Multilaboratory changes in fHb concentration for the three test conditions and their respective controls are displayed in Fig. 3. In all cases, the hemolysis values were above the minimal detection level of 1–2 mg/dL for the fHb concentration assay (33). For the 5- and 6-L/min sudden-contraction nozzle inlet flow conditions, the hemolysis levels were two to nine times greater than in their corresponding control loops. In contrast, the gradual cone nozzle inlet test condition at 6 L/min did not generate significantly more hemolysis than the control loop. This result indicates that the gradual cone inlet and the 4-mm throat of the nozzle produced minimal damage to RBCs at the highest tested flow rate. The two bars denoted by symbols in Fig. 3 each contain a single data outlier as specified by Grubbs' test. These outliers were likely caused by procedural errors or blood contamination and were not included in the subsequent analysis and histograms (Fig. 4).

The flow-induced hemolysis caused only by the nozzle ($MIH_{nozzle}$) was calculated by subtracting the blood damage generated in the corresponding control loop. Figure 4A shows the $MIH_{nozzle}$ results for each test condition and laboratory. There were no statistical differences among the hemolysis levels measured at the three laboratories when the sudden-contraction geometry was at the nozzle inlet at 5 and 6 L/min ($P > 0.09$). However, for the test condition that caused the least amount of hemolysis (gradual cone inlet condition at 6 L/min), Laboratory 3 generated a higher level of hemolysis than Laboratory 2 ($P = 0.03$). The low $MIH_{nozzle}$ values for the gradual cone inlet indicate that this nozzle configuration generates comparable hemolysis to the corresponding control loop.

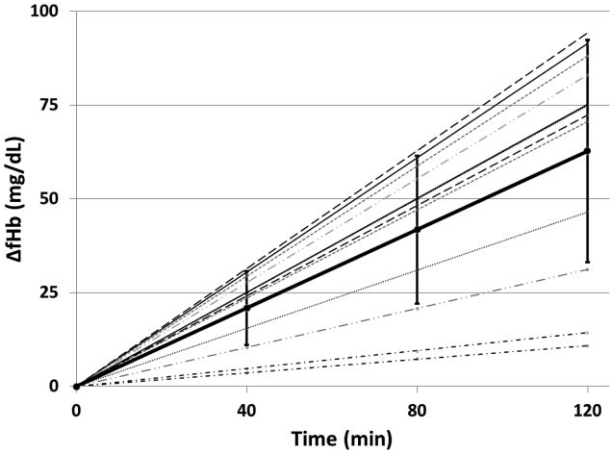


**FIG. 2.** Changes in plasma free hemoglobin concentration for bovine blood during 120 min of testing for Laboratory 1, showing all 12 individual tests of the 6-L/min sudden-contraction nozzle inlet condition ($r^2 > 0.94$ for each individual test). The bold line represents the mean ± SD values at each blood sample time point, and similar trend lines indicate which experiments used the same blood pool on 2 consecutive test days.

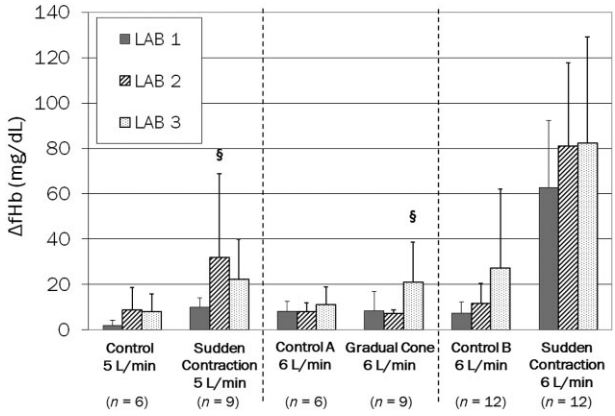


**FIG. 3.** Change in plasma free hemoglobin concentration for bovine blood after 120 min of testing in nozzle and control conditions for three laboratories. Values are shown as mean ± SD for each laboratory, and the number of replicates per lab ($n$) is indicated for each test condition. §A single outlier was present and included in the specified data set.

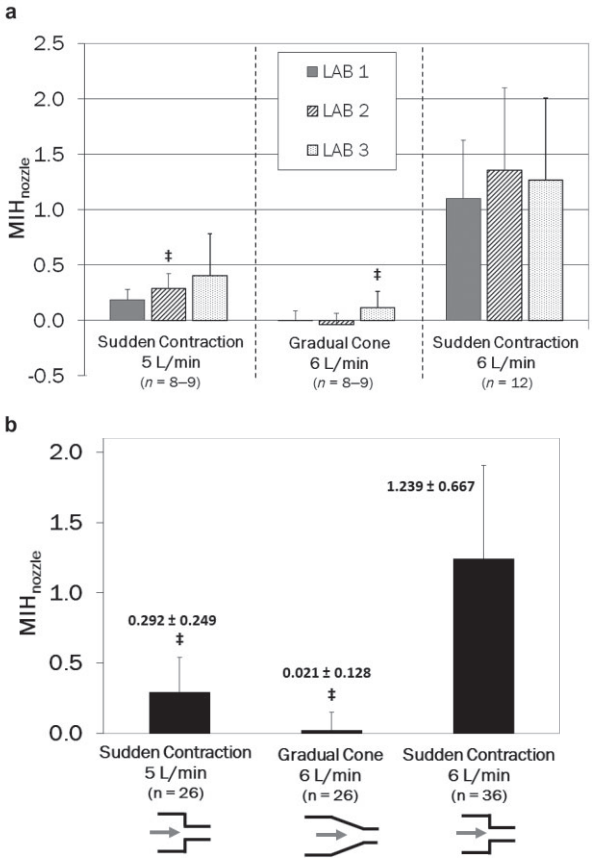


**FIG. 4.** MIH values for the three nozzle test conditions after subtraction of the control loop MIH values (A) for each laboratory and (B) averaged for the three laboratories. ‡A single outlier was removed from the specified data set ($n$ = total number of replicates).

The collated hemolysis values from the three laboratories for each nozzle test condition were significantly different from one another (Fig. 4b, $P < 0.001$). Despite having similar nozzle throat Reynolds numbers and afterload pressures at a flow rate of 6 L/min (Table 2), the sharp corner geometry of the sudden-contraction inlet produced much more hemolysis ($MIH_{nozzle} = 1.239 \pm 0.667$, $n = 36$) than the gradual cone inlet condition ($MIH_{nozzle} = 0.021 \pm 0.128$, $n = 26$). Flow rate was also a major factor in hemolysis generation; the sudden-contraction nozzle inlet caused more hemolysis at 6 L/min than at 5 L/min ($MIH_{nozzle} = 0.292 \pm 0.249$, $n = 26$). The ratio of hemolysis values between the test conditions (mean ± SD) was also calculated. Relative to the 5-L/min sudden-contraction inlet condition, the 6 L/min sudden-contraction inlet generated on average $4.24 \pm 0.79$ times more hemolysis, while the 6-L/min conical inlet generated approximately 14 times less (i.e., ratio = $0.07 \pm 0.09$).

The same relative trends in hemolysis generation for each test condition were observed independent of parameter or index (ΔfHb, NIH, MIH). There were significant Pearson product-moment correlation coefficients (r) for ΔfHb versus NIH (0.994), ΔfHb versus MIH (0.988), and NIH versus MIH (0.997).

Three types of variability associated with the in vitro hemolysis testing were determined in this study: (i) repeatability—a comparison of identical tests performed on the same day with the same test loop and using the same blood pool; (ii) intralaboratory variability—variability at each test facility when performing the same test with different blood pools on different days; and (iii) interlaboratory variability—a comparison of the differences in hemolysis values across the three test facilities. The repeatability for the sudden-contraction nozzle inlet hemolysis tests at both 5 and 6 L/min, in terms of the percent coefficient of variation, was 18% ($n = 14$). Some of the results used to assess repeatability were collected during preliminary reproducibility testing of the models. The intralaboratory variability of the $MIH_{nozzle}$ values for the three laboratories ranged from 47 to 94% (from Fig. 4A). Hence, the inherent variability associated with repeat experiments on a single day was significantly less than the intralaboratory variability established over multiple days of testing with different blood pools. Additionally, it was determined that intralaboratory variability was greater than the interlaboratory variability (54–85%) using a random-effect model ($F > 100$, $P < 0.001$).

To estimate the contribution of flow-related uncertainties to the overall variability in the hemolysis results, an error propagation analysis was performed post hoc. We estimated that variability in viscosity, flow rate, and density measurements could lead to a 23% uncertainty in the Reynolds number. After determining the viscous and Reynolds stresses in the nozzle using a CFD simulation, a modified Grigioni (Lagrangian) blood damage model (34) was used to predict that the variability in these flow-related parameters could only account for up to 15% CV in the hemolysis index at each test condition. As the intra-laboratory hemolysis variability ranged from 47 to 94% CV, this indicates that the combined uncertainty associated with the experimentally measured flow rate, viscosity, and, to a lesser extent, density accounted for less than a third of the overall intra- and interlaboratory variability in hemolysis.

The RBC rocker bead mechanical fragility test was used to determine whether the MFI of each blood pool correlated with the hemolysis produced

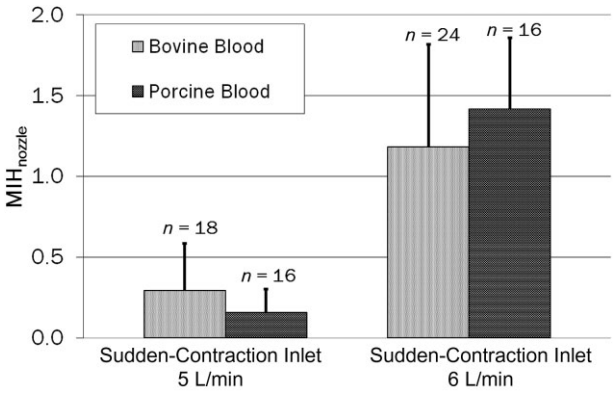


**FIG. 5.** Comparison of the MIH between bovine and porcine blood for two nozzle test conditions after subtraction of the control loop MIH values at two laboratories. Values are shown as mean ± SD ($n$ = total number of replicates per test condition).

by the nozzle. For each of the three laboratories, the mean RBC MFI values for 36% hematocrit bovine blood were $0.56 \pm 0.10$, $0.45 \pm 0.12$, and $0.62 \pm 0.18$, which were significantly different from one another ($P < 0.02$). With a coefficient of variation of only 4% ($n = 30$), the repeatability of the RBC mechanical fragility tests using the same blood on the same test day at each laboratory was very high. The intralaboratory variability (% CV) ranged from 17 to 29% and the interlaboratory variability was 28% for this test, and there was no significant difference in MFI between the first and second test days ($P > 0.05$). Overall, there was not a clear correlation between the MFI of the blood on each test day and the amount of hemolysis generated by the three separate nozzle test conditions ($P > 0.05$).

A subset of experiments was also conducted by two laboratories using both porcine and bovine blood to determine if blood species affected hemolysis generation in the MFI test and the nozzle model. As there was no interlaboratory difference in the nozzle hemolysis results ($P > 0.08$), the data were collated for the two laboratories. Porcine RBCs better match the rheological and morphological properties of human RBCs, including a larger mean corpuscular volume, in comparison to bovine blood cells (12,36). The RBC mechanical fragility tests showed that bovine blood had a higher mean MFI than porcine blood ($0.54 \pm 0.15$ vs. $0.42 \pm 0.06$, respectively; $P < 0.01$; Table 1), perhaps due to a slightly higher concentration of protective total protein in the porcine blood (37). While the MFI test indicated that bovine blood may be more sensitive to damage, Fig. 5 shows that there was no statistical difference in flow-induced hemolysis between porcine and bovine blood (both at 36% Hct) using the FDA nozzle model with the sudden-contraction inlet at flow rates of 5 and 6 L/min ($P = 0.57$). There was, however, a statistical difference between the species for the relative ratio of hemolysis generated at the 6-L/min versus the 5-L/min condition ($P = 0.03$). The hemolysis ratio was $8.93 \pm 2.07$ for porcine blood and $4.02 \pm 1.00$ for bovine blood.

## DISCUSSION

As in vitro hemolysis test results are a function of many different factors such as blood species, blood management, temperature, and test model (8,38,39) and can be laboratory-dependent, this multi-laboratory study was conducted to evaluate in vitro hemolysis testing techniques and to generate experimental data to assist in the implementation of CFD for the blood damage safety evaluation of medical devices. In previous studies, similar nozzle models and test conditions were used (i.e., bovine blood tested at 5 or 6 L/min through 10–11-mm-diameter inlet tubes past sharp-cornered and tapered inlets into constricting 4–5-mm-diameter throats that were 12–15 mm in length), but the hemolysis results differed by a factor of approximately 50 (26,27). This discrepancy reflects the difficulty in comparing in vitro hemolysis test results across different studies when there is a paucity of repeated tests and differences in temperature, pump afterload, pump operation, blood volume, flow rate, loop components, hematocrit, blood species, blood drawing methods, and anticoagulation. As another example, literature values of NIH for the Biomedicus BP-80 pump (Medtronic, Minneapolis, MN, USA) tested under similar operating conditions range from 0.0007 to 0.018 g/100 L, with individual study coefficients of variation ranging from 18 to 94% (40–42). Advantages of the current study are the following: (i) the nozzle model was comparatively tested at three different laboratories and had similar pressure losses and hemolysis results, (ii) many test replicates were performed using both bovine and porcine blood, (iii) the flow-induced nozzle hemolysis level was obtained by correcting for the background hemolysis caused by the pump and loop components, and (iv) all testing and nozzle model parameters are provided in this text.

As expected, the sudden-contraction inlet configuration caused significantly higher hemolysis than the gradually tapering cone inlet, suggesting that the sharp corner geometry of the sudden-contraction inlet was the primary source of blood damage. As hemolysis testing was performed below the threshold for cavitation formation in this study, any measured

RBC lysis was attributed to flow-generated stresses. As shown by CFD analysis, the sudden-contraction configuration produced high viscous shear stresses at the sharp corner and large variations in the wall shear stress magnitudes and distributions (25). Furthermore, the wall shear stresses associated with the gradual cone inlet condition were smaller than at the sudden-expansion outlet and did not cause much hemolysis (24,25). The parameters used in this study to report hemolysis (i.e., plasma free hemoglobin, NIH, and MIH) did not impact data interpretation because the blood flow rate, hematocrit and total hemoglobin levels, blood volume, and sampling time were carefully controlled. Therefore, irrespective of which hemolysis parameter is used, the results displayed in Fig. 4B (e.g., MIH) may be used to help develop and verify predictive CFD models of blood damage as long as the variability in the hemolysis results is also taken into consideration. However, considering that blood damage test results may vary due to test temperature, length between blood collection and use, anticoagulation, blood pH, oxygenation, and glucose levels (8), it should be noted that the hemolysis results reported here are specific for the blood parameters used in our testing (i.e., passive-flow nozzle model with a 4 mm throat, bovine and porcine blood cold-stored in some cases for up to 80 h after withdrawal, ACDA anticoagulation, blood test temperature of 25°C, 36% hematocrit).

Another important aspect of this study was to examine the variability associated with in vitro hemolysis experiments. To account for the high variability in the test results and to conduct robust statistical analyses, a large number of replicates were necessary. By utilizing three laboratories, a combined total of 26–36 data points were accumulated at each nozzle test condition. While identical clinical blood pumps were used and a standard operating procedure was followed, subtle differences in experimental technique (including blood collection, handling and sampling), blood source and age, animal-to-animal variation, equipment calibration, variable loop and reservoir configurations, and cleaning procedures still may have contributed to the interlaboratory variability shown in Fig. 3. Additionally, much of the intralaboratory variability could be attributed to inherent differences in blood cell fragility not captured by the rocker bead fragility test, performance changes of the individual flow loop components, de-airing inconsistencies, loop construction alterations, or variations in operating the systems. In this study, some day-to-day variability was compensated for by subtracting the hemolysis measured in a paired control flow loop (Fig. 4). This was important as the parallel tests showed a significant positive correlation between the hemolysis caused by the control loop and its corresponding nozzle test loop ($P < 0.002$).

A comparison between bovine and porcine blood was performed using the RBC mechanical fragility (rocker bead) test and hemolysis tests of two nozzle flow conditions (by two laboratories), as both blood types are readily available in large quantities and often used for in vitro medical device testing. An important area of investigation is determining how in vitro hemolysis results obtained with animal blood can be extrapolated to human clinical situations. Porcine blood is thought to be more relevant than bovine blood for in vitro blood damage testing (12). The differences in RBC size and fragility of bovine and porcine blood are likely to be more noticeable in smaller-scale models, such as orifice jet flow models or shearing devices with small gaps (12,39), as only a small percentage of the RBCs may contact the walls or be exposed to the elevated shear stresses at the sudden-contraction inlet during a single pass (25).

The RBC mechanical fragility tests (with rocked beads) varied between the laboratories but indicated that bovine RBCs were more fragile than porcine RBCs (Table 1). The sudden contraction nozzle inlet results showed no significant difference in RBC damage between bovine and porcine blood at the 5- and 6-L/min conditions (Fig. 5), yet the relative ratio of hemolysis between flow rates suggests otherwise ($P = 0.03$). This discrepancy should not be misconstrued as proof that porcine blood was more sensitive than bovine blood for the nozzle model. For the 5-L/min sudden-contraction inlet condition, bovine blood actually yielded a higher average hemolysis value than did porcine blood. The relative ratio calculations were unduly impacted by the relatively low blood damage levels at 5 L/min for both species. Hence, to properly determine differences in blood fragility between different species, more testing conditions with a wider range of hemolysis values are required.

The RBC mechanical fragility test also allowed for the assessment of test variability in a simple system that did not include a pump or recirculating flow loop. The RBC mechanical fragility test results were highly repeatable (4% CV) when bovine blood from the same pool was used, with individual intralaboratory variability about half that of the nozzle experiments. The statistically significant difference in bovine RBC MFI values among laboratories is likely a combination of both blood- (source, collection method) and laboratory-specific variability. While a clear correlation was not observed between RBC MFI and flow-induced hemolysis, the rocker bead test can still be

useful as a measure of quality control within laboratories to identify highly fragile blood cells prior to testing (43). It should be noted that the mechanisms for blood damage in the RBC mechanical fragility test (with laminar flow conditions and multiple bead-surface collisions) should be markedly different than for the turbulent flow conditions within the experimental nozzle recirculating flow loop.

## CONCLUSIONS

A multilaboratory in vitro study was conducted to generate hemolysis and pressure loss data for a benchmark nozzle model. The hemolysis levels for the three test conditions were similar across the independent laboratories, suggesting that the major factors affecting red blood cell damage were controlled in the study. Despite high intralaboratory variability, statistically significant differences among the three test conditions were observed, with the sudden-contraction nozzle entrance causing the most blood damage. Because the hemolysis experiments were performed using a well-defined model, these results may help to support, validate, and advance the development of predictive computational models of blood damage, as long as the dependences on the specific blood parameters and variability of the hemolysis results are taken into consideration. Further studies are needed on other models and devices over a range of operating conditions to provide the much-needed hemolysis data that can be used to augment computational predictions of blood damage.

**Acknowledgments:** This study was supported by the US Food and Drug Administration's Critical Path Initiative. From the FDA, we would like to thank Dr. Meijuan Li for providing invaluable statistical analyses, Dr. Prasanna Hariharan and Gavin D'Souza for performing computational simulations and error propagation analyses, Jean Rinaldi for reviewing the manuscript, and Drs. Sandy Stewart and Qijin Lu for technical support. We recognize and appreciate the support of Brittany Arcuri, Christine Flick, and Elizabeth Endrizzi for assisting with experiments at the Cleveland Clinic, and Andrew Wearden and Charles Lutzow for helping with experimental data collection at the University of Pittsburgh. We would also like to acknowledge the efforts of Dr. Steven Day, Matthew Giarra, and Alex Ship at the Rochester Institute of Technology in fabricating the nozzle models. Lastly, the authors would also like to thank Dr. Kurt Dasse, Farzad Parsaie, and the team at Levitronix LLC for providing centrifugal blood pumps for this study through a Material Transfer Agreement. Any mention of commercial products and/or manufacturers does not imply endorsement by the US Department of Health and Human Services.

**Conflict of Interest:** The authors declare that they have no conflicts of interest.

## REFERENCES

1. Kim NJ, Diao C, Ahn KH, Lee SJ, Kameneva MV, Antaki JF. Parametric study of blade tip clearance, flow rate, and impellerspeed on blood damage in rotary blood pump. *Artif Organs* 2009;33:468–74.
2. Dasi LP, Simon HA, Sucosky P, Yoganathan AP. Fluid mechanics of artificial heart valves. *Clin Exp Pharmacol Physiol* 2009;36:225–37.
3. Kennedy C, Angermuller S, King R, et al. A comparison of hemolysis rates using intravenous catheters versus venipuncture tubes for obtaining blood samples. *J Emerg Nurs* 1996;22:566–9.
4. Iwahashi H, Yuri K, Nosé Y. Development of the oxygenator: past, present, and future. *J Artif Organs* 2004;7:111–20.
5. Rother RP, Bell L, Hillmen P, Gladwin MT. The clinical sequelae of intravascular hemolysis and extracellular plasma hemoglobin. *J Am Med Assoc* 2005;293:1653–62.
6. ASTM International. ASTM Standard F1841-97: standard practice for assessment of hemolysis in continuous flow blood pumps. West Conshohocken, PA: ASTM International, 2013. doi: 10.1520/F1841-97R13.
7. Food and Drug Administration Center for Devices and Radiological Health. Guidance for cardiopulmonary bypass oxygenators 510(k) submissions: final guidance for industry and FDA staff. Silver Spring, MD: Food and Drug Administration, 2000.
8. Mueller MR, Schima H, Engelhardt H, et al. In vitro hematological testing of rotary blood pumps: remarks on standardization and data interpretation. *Artif Organs* 1993;17:103–10.
9. Leverett LB, Hellums JD, Alfrey CP, Lynch EC. Red blood cell damage by shear stress. *Biophysics J* 1972;12:257–73.
10. Hellums JD, Brown CH. Blood cell damage by mechanical forces. In: Hwang NHC, Normann NA, eds. *Cardiovascular Flow Dynamics and Measurements*. Baltimore: University Park Press, 1977;799–823.
11. Sutera SP. Flow-induced trauma to blood cells. *Circ Res* 1997;41:2–8.
12. Paul R, Apel J, Klaus S, Schügner F, Schwindke P, Reul H. Shear stress related blood damage in laminar Couette flow. *Artif Organs* 2003;27:517–29.
13. Zhang T, Taskin E, Fang HB, et al. Study of flow-induced hemolysis using novel couette-type blood-shearing devices. *Artif Organs* 2011;35:1180–6.
14. Gu L, Smith WA. Evaluation of computational models for hemolysis evaluation. *ASAIO J* 2005;51:202–7.
15. Bluestein D. Research approaches for studying flow-induced thromboembolic complications in blood recirculating devices. *Expert Rev Med Dev* 2004;1:65–80.
16. Yoganathan A, Chandran K, Sotiropoulos F. Flow in prosthetic heart valves: state-of-the-art and future directions. *Ann Biomed Eng* 2005;33:1689–94.
17. Fraser KH, Taskin ME, Griffith BP, Wu ZJ. The use of computational fluid dynamics in the development of ventricular assist devices. *Med Eng Phys* 2011;33:263–80.
18. Goubergrits L. Numerical modeling of blood damage: current status, challenges and future prospects. *Expert Rev Med Devices* 2006;3:527–31.

19. Forstrom RJ. *A New Measure of Erythrocyte Membrane Strength: The Jet Fragility Test*. Minneapolis, MN: University of Minnesota, 1969.
20. Jikuya T, Tsutui T, Shigeta O, Sankai Y, Mitsui T. Species differences in erythrocyte mechanical fragility: comparison of human, bovine, and ovine cells. *ASAIO J* 1998;44:M452–5.
21. Takami Y, Nakazawa T, Makinouchi K, et al. Hemolytic effect of surface roughness of an impeller in a centrifugal blood pump. *Artif Organs* 1997;21:686–90.
22. Naito K, Mizuguchi K, Nose Y. The need for standardizing the index of hemolysis. *Artif Organs* 1994;18:7–10.
23. Hariharan P, Giarra M, Reddy V, et al. Multi-laboratory particle image velocimetry analysis of the FDA benchmark nozzle model to support validation of computational fluid dynamics simulations. *J Biomech Eng* 2011;133:041002–1-14.
24. Stewart SFC, Paterson EG, Burgreen GW, et al. Assessment of CFD performance in simulations of an idealized medical device—results of FDA's first computational interlaboratory study. *Cardiovasc Eng Tech* 2012;3:139–60.
25. Stewart S, Hariharan P, Paterson E, et al. Results of FDA's first interlaboratory computational study of a nozzle with a sudden contraction and conical diffuser. *Cardiovasc Eng Technol* 2013;4:1–18.
26. Umezu M, Fujimasu H, Yamada T, et al. Fluid dynamic investigation of mechanical blood hemolysis. In: Akutsu T, Koyanagi H, eds. *Heart Replacement: Artificial Heart 5*. Tokyo: Springer, 1996;327–40.
27. Tamagawa M, Akamatsu T, Saitoh K. Prediction of hemolysis in turbulent shear orifice flow. *Artif Organs* 1996;20: 553–9.
28. Umezu M, Yamada T, Fujimasu H, et al. Effects of surface roughness on mechanical hemolysis. *Artif Organs* 1996;20: 575–8.
29. Hess JR. An update on solutions for red cell storage. *Vox Sang* 2006;91:13–9.
30. Kameneva MV, Antaki JF, Konishi H, et al. Effect of perfluorochemical emulsion on blood trauma and hemorheology. *ASAIO J* 1994;40:M576–9.
31. Gu L, Smith WA, Chatzimavroudis GP. Mechanical fragility calibration of red blood cells. *ASAIO J* 2005;51:194–201.
32. Cripps C. Rapid method for the estimation of plasma haemoglobin levels. *J Clin Pathol* 1968;21:110–2.
33. Malinauskas RA. Plasma hemoglobin measurement techniques for the in vitro evaluation of blood damage caused by medical devices. *Artif Organs* 1997;21:1255–67.
34. Grigioni M, Mobiducci U, D'Avenio G, Benedetto GD, Gaudio CD. A novel formulation for blood trauma prediction by a modified power-law mathematical model. *Biomech Model Mechanobiol* 2005;4:249–60.
35. Giersiepen M, Wurzinger LJ, Opitz R, Reul H. Estimation of shear stress-related blood damage in heart valve prostheses—in vitro comparison of 25 aortic valves. *Int J Artif Organs* 1990;13:300–6.
36. Windberger U, Bartholovitsch A, Plasenzotti R, Korak KJ, Heinze G. Whole blood viscosity, plasma viscosity and erythrocyte aggregation in nine mammalian species: reference values and comparison of data. *Exp Physiol* 2003;88:431–40.
37. Kameneva MV, Antaki JF, Yeleswarapu KK, Watach MJ, Borovetz HS. Plasma protective effect on red blood cells exposed to mechanical stress. *ASAIO Journal* 1997;43: M571–5.
38. Kameneva MV, Burgreen GW, Kono K, Repko B, Antaki JF, Umezu M. Effects of turbulent stresses upon mechanical hemolysis: experimental and computational analysis. *ASAIO J* 2004;50:418–23.
39. Klaus S, Körfer S, Mottaghy K, Reul H, Glasmacher B. In vitro blood damage by high shear flow: human versus porcine blood. *Int J Artificial Organs* 2002;25:306–12.
40. Naito K, Suenaga E, Cao ZL, et al. Comparative hemolysis study of clinically available centrifugal pumps. *Artif Organs* 1996;20:560–3.
41. Steines D, Westphal D, Göbel C, Reul H, Rau G. Platelet function and hemolysis in centrifugal pumps: in vitro investigations. *Int J Artif Organs* 1999;22:559–65.
42. Kawahito K, Nose Y. Hemolysis in different centrifugal pumps. *Artif Organs* 1997;21:323–6.
43. Raval JS, Waters JH, Seltsam A, et al. The use of the mechanical fragility test in evaluating sublethal RBC injury during storage. *Vox Sang* 2010;99:235–31.